J. Innovative Eng. Nat. Sci., vol. 6, no. 2, pp. 368-376, 2026.
http://doi.org/10.61112/jiens.1948512

Journal of Innovative Engineering and Natural Science
(Yenilikçi Mühendislik ve Doğa Bilimleri Dergisi)
https://dergipark.org.tr/en/pub/jiens

Original Paper

Evaluation of the thermodynamic behavior of white benzoin via inverse gas chromatography

Ayse Erdogan Cakar[a,*]

[a]*Yildiz Technical University, Department of Chemistry, Faculty of Arts & Sciences, Esenler, Istanbul, 34220, Turkey*

ARTICLE INFO

Article history:
Received May 10, 2026
Received in revised form June 21, 2026
Accepted July 17, 2026

Available online

Keywords:
White Benzoin
Thermodynamic Properties
Inverse Gas Chromatography

ABSTRACT

This study, the thermodynamic properties of white benzoin (WB) were examined by the inverse gas chromatography (IGC) method. To evaluate the polymer-solvent interaction parameters, the specific retention volume of the solvents, V_g^0 values were determined using various nonpolar and polar solvents in the temperature range of 373.2 –398.2 K. Then, from these data, the values of the Flory-Huggins theory polymer-solvent interaction parameters, χ_{12}^{∞}, equation of state theory, polymer-solvent interaction parameters, χ_{12}^{*}, effective exchange energy parameters, X_{eff}, and also the partial molar heat of mixing at infinite dilution of solvent, $\Delta\bar{H}_1^{\infty}$, the molar heat of vaporization of solvent, $\Delta\bar{H}_v$, and the partial molar heat of sorption of solvent, $\Delta\bar{H}_1^{s}$ were calculated. The results obtained were discussed.

I. INTRODUCTION

Benzoin, also known as jawi or Styrax, is the resin of a perennial plant from the Styracaceae family that grows in the warm climates of the northern hemisphere. Since ancient times, it has been used as incense and fragrance due to its pleasant scent reminiscent of vanilla and willow. With over 150 varieties used for this purpose, benzoin can be broadly categorized into two main types: Siam benzoin and Sumatra benzoin. Sumatra benzoin contains higher levels of cinnamic acid and cinnamate than Siam benzoin, while Siam benzoin has a higher benzoic acid content. This variation in composition is due to the region where the tree grow [1, 2].

Benzoin resins are a white/yellow resin that oozes from a small incision made in the tree trunk. The resin then hardens and oxidizes, turning a reddish-brown color. Subsequent harvests have a higher antioxidant content, thought to be due to the high amount of phenolic and flavonoid compounds in their composition. Its chemical structure generally consists of cinnamyl cinnamate, methyl cinnamate, cinnamic acid, benzyl cinnamate, benzoic acid, small amounts of vanillin, small amounts of volatile acids, and amorphous resins. Free benzoic and cinnamic acids, along with their esters such as coniferyl and p-coumaryl alcohols, are present in varying amounts, and some higher molecular weight compounds such as pinoresinol are also present in its structure [1-4].

In inverse gas chromatography (IGC), considered an extension of conventional gas chromatography, this difference arises from the inversion of phases. In conventional gas chromatography, the phase within the column is fixed. The sample is characterized by observing the retention time and peak area of the injected volatile component, whose properties are unknown. However, in IGC, the sample to be characterized is loaded into the column, and known volatile probes such as heptane and methyl acetate are injected into the column to investigate

*Corresponding author. Tel.: +90-212-383-4130; e-mail: aecakar@yildiz.edu.tr

what happens at the interface between the sample and the gas phase [5-7]. The reason for choosing polar and non-polar probes is to try to gain a broader understanding of the surfaces [5].

IGC is divided into two types, infinite dilution and finite concentration, depending on the amount of probe injected. In infinite dilution, only a small amount of probe, just enough for the detector to detect, is sent to the detector. In finite concentration, only a few mL of probe is sent to the detector for analysis [6, 7] Dispersive surface energy, nanoroughness, and acid-base properties are determined using infinitely dilute concentrations. This allows for the characterization of surface area distributions with different energies and surface heterogeneity [8]. The surface of any material can be subjected to non-polar (dispersive), polar (specific), and surface interactions such as acid-base interactions [9].

II. EXPERIMENTAL METHOD / TEORETICAL METHOD

In inverse gas chromatography, the time during which probe molecules remain in the column due to intermolecular forces between the stationary phase and the probe molecules is defined as the retention time. The volume of carrier gas passing through the column during this retention time is called the net retention volume. To describe the solvent-sample interaction, the retention volume at which the column pressure is set to zero is used, and this is called the specific retention volume V_g^0 [7, 10, 11]. Thanks to the attention paid to the stationary excess within the column by inverse gas chromatography, fundamental thermodynamic properties such as infinite dilution activity coefficients, Flory-Huggins interaction parameters, and solubility parameters can be elucidated [12].

$$V_g^0 = \frac{Q \cdot (t_R - t_A) \cdot J \cdot 273.2}{(T_r \cdot w)} \tag{1}$$

where Q denotes the carrier gas flow rate measured at room temperature (T_r), t_R and t_A are the retention times of the solvent probe and air, respectively, w represents the mass of the polymer packed into the column. Because the carrier gas is compressible, the outlet volume measured at the end of the column does not accurately represent the true retention volume. As the carrier gas travels through the column, the pressure decreases continuously, causing gradual expansion of the gas and a corresponding increase in volumetric flow rate along the column length. To account for this effect, the James–Martin compressibility correction factor (J) is applied. This correction factor depends on the column inlet pressure; P_g and outlet pressure P_c. Under typical experimental conditions, the outlet pressure is assumed to be equal to atmospheric pressure.

$$J = \left(\frac{3}{2}\right) \cdot \left[\frac{\left(\frac{P_g}{P_c}\right)^2 - 1}{\left(\frac{P_g}{P_c}\right)^3 - 1}\right] \tag{2}$$

The Flory–Huggins interaction parameter (χ_{12}^{∞}) and the equation-of-state interaction parameter (χ_{12}^{*}) were determined from Equations (3) and (4), respectively [13-15].

$$\chi_{12}^{\infty} = \ln\left(\frac{273.2 \cdot R \cdot v_2}{p_1^0 \cdot V_g^0 \cdot V_1^0}\right) - 1 - \frac{p_1^0 \cdot (B_{11} - V_1^0)}{R \cdot T} \quad (3)$$

The interaction parameter in the equation-of-state theory, χ_{12}^{*}, at infinite dilution of the solvent is defined by the following equation [16-18]:

$$\chi_{12}^{*} = \ln\left(\frac{273.2 \cdot R \cdot v_2^{*}}{p_1^0 \cdot V_g^0 \cdot V_1^{*}}\right) - 1 - \frac{p_1^0 \cdot (B_{11} - V_1^0)}{R \cdot T} \quad (4)$$

where R is the universal gas constant; P_1^0 and B_{11} denote the saturated vapor pressure and the second virial coefficient of the solvent vapor, respectively. B_{11} of the deviation of the vapor phase solvent from the ideality that is evaluated by:

$$B_{11} = \frac{\left(0.430 - 0.886(T_c/T) - 0.694(T_c/T)^2 - 0.037(n-1)(T_c/T)^{9/2}\right)}{V_c} \quad (5)$$

where n is the number of carbon atoms in solvents (for permanent gases, n=1 and the last term become zero); T_c is the critical temperature of the solvents; and V_c is the critical molar volume of the solvent. V_1^0 is the molar volume of the solvent at temperature T; and v_2 and v_2^{*} represent the specific volume and the specific hardcore volume of the polymer packed in the column, respectively [10, 19-21]. Moreover, V_1^{*} is the molar hardcore volume of the solvent. According to the equation-of-state theory, the effective exchange energy parameter $(\chi_{eff})$is expressed by Equation (6):

$$R \cdot T \cdot \chi_{12}^{*} = p_1^{*} \cdot V_1^{*}\left\{3T_{1r} \cdot ln\left[\left(v_{1r}^{1/3} - 1\right)/\left(v_{2r}^{1/3} - 1\right)\right] + v_{1r}^{-1} - v_{2r}^{-1} + \chi_{eff}/P_1^{*} \cdot v_{2r}\right\} \quad (6)$$

where p_1^{*} is the characteristic pressure; v_{1r} and v_{2r} are the reduced volumes of the solvent and polymer, respectively; and T_{1r} is the reduced temperature of the solvent [22].

When the plot of $\ln V_g^0$ versus $1/T$ (retention diagram) exhibits a linear relationship, the system is assumed to be at equilibrium within the studied temperature range. Under these conditions, the partial molar heat of sorption of the solvent by the solute ($\Delta\bar{H}_1^s$) can be determined from the slope of the straight line using Equation (7) [23].

$$\Delta\bar{H}_1^s = -R\frac{\partial\left(ln\, V_g^0\right)}{\partial(1/T)} \quad (7)$$

The weight fraction activity coefficient at infinite dilution (Ω_1^{∞}), which is used to calculate the thermodynamic parameters. Also, the partial molar heat of mixing, $\Delta\bar{H}_1^{\infty}$, can be calculated (equation (9)) for the temperature range over which the plot of $ln\,\Omega_1^{\infty}$ versus $1/T$ is linear.

$$ln(\Omega_1^{\infty}) = \ln\left(\frac{273.2 \cdot R}{V_g^o \cdot P_1^o \cdot M_1}\right) - \left(\frac{P_1^o \cdot (B_{11} - V_1^o)}{R \cdot T}\right) \quad (8)$$

where, M_1 is the molecular weight of the solvent.

$$\Delta\bar{H}_1^{\infty} = R\frac{\partial(ln\,\Omega_1^{\infty})}{\partial(1/T)} \quad (9)$$

The molar heat of vaporization of the solvent, $\Delta\bar{H}_v$, is related to $\Delta\bar{H}_1^s$ and $\Delta\bar{H}_1^{\infty}$ as in equation (8);

$$\Delta\bar{H}_v = \Delta\bar{H}_1^{\infty} - \Delta\bar{H}_1^s \quad (10)$$

2.1 Experimental

2.1.1. Materials

The support material, Chromosorb-W (AW-DMCS treated, 80/100 mesh), was supplied by Merck AG Inc., Germany. Silane-treated glass wool, used to plug both ends of the chromatographic column, was obtained from Alltech Associates Inc., USA. WB was sourced from a local market in Bahrain. The abbreviations, suppliers, purity levels (mass fraction), and CAS registry numbers of all solvents used in the IGC experiments are listed in Table 1.

Table 1. Abbreviation, source, purity, and CAS number of the solvents

Chemical name	Abbreviation	Source	Purity	CAS number
n-octane	O	Merck	≥ 0.990	111-65-9
n-nonane	N	Merck	≥ 0.990	111-84-2
n-decane	D	Merck	≥ 0.995	124-18-5
n-undecane	UN	Merck	≥0.99	1120-21-4
n-dodecane	DD	Merck	≥0.99	112-40-3
n-tridecane	TD	Merck	≥0.99	629-50-5
n-butyl acetate	nBA	Supelco	≥0.995	123-86-4
i-butyl acetate	iBA	Sigma-Aldrich	≥0.98	110-19-0
Chlorobenzene	CB	Merck	≥0.99	108-90-7
Ethyl acetate	EA	Merck	≥ 0.995	141-78-6
i-propylbenzene	iPB	Sigma-Aldrich	≥0.98	98-82-8
n-propylbenzene	nPB	Sigma-Aldrich	≥0.99	103-65-1
Ethylbenzene	EB	Sigma-Aldrich	≥0.99	100-41-4
Toluene	T	Supelco	≥0.998	108-88-3

IGC measurements were performed using an Agilent Technologies 6890N gas chromatograph equipped with a thermal conductivity detector (TCD), USA. The chromatographic column, consisting of stainless-steel tubing with an outer diameter of 3.2 mm and a length of 0.5 m, was purchased from Alltech Associates Inc., USA. A total of about 0.6 g of packing material (approximately 20% by weight of WB) was placed in the column. To remove residual moisture, the benzoins were first dried in a vacuum oven at 50 °C for 24 hours before being used as the stationary phase. They were then dissolved in ethanol, and Chromosorb W was gradually added with continuous stirring. Stirring was maintained until the solvent had completely evaporated. The resulting stationary phase was obtained in powder form and further dried in a vacuum oven at 60 °C for 48 hours to ensure complete removal of any remaining solvent.

A 1 µL Hamilton syringe was used to inject solvent into the colon, and a 10 µL syringe was used to inject air; 0.2-0.3 µL of solvent was drawn with the 1 µL syringe and completed to 1 µL with air. At each column temperature, at least four consecutive solvent injections were carried out. The retention time was determined by averaging the

results of these four measurements. The carrier gas flow rate was experimentally set between 3–4 $cm^3.min^{-1}$ and maintained constant throughout the IGC experiments.

2.2 Bulk properties

Thermodynamic equilibrium calculations for the polymer–solvent system were performed within the temperature range of 373.2–398.2 K. For this purpose, retention diagrams of polar and non-polar solvents were plotted and are presented in Figures 1 and 2, respectively. The linearity observed in the retention diagrams over the studied temperature range indicates that thermodynamic equilibrium was attained.

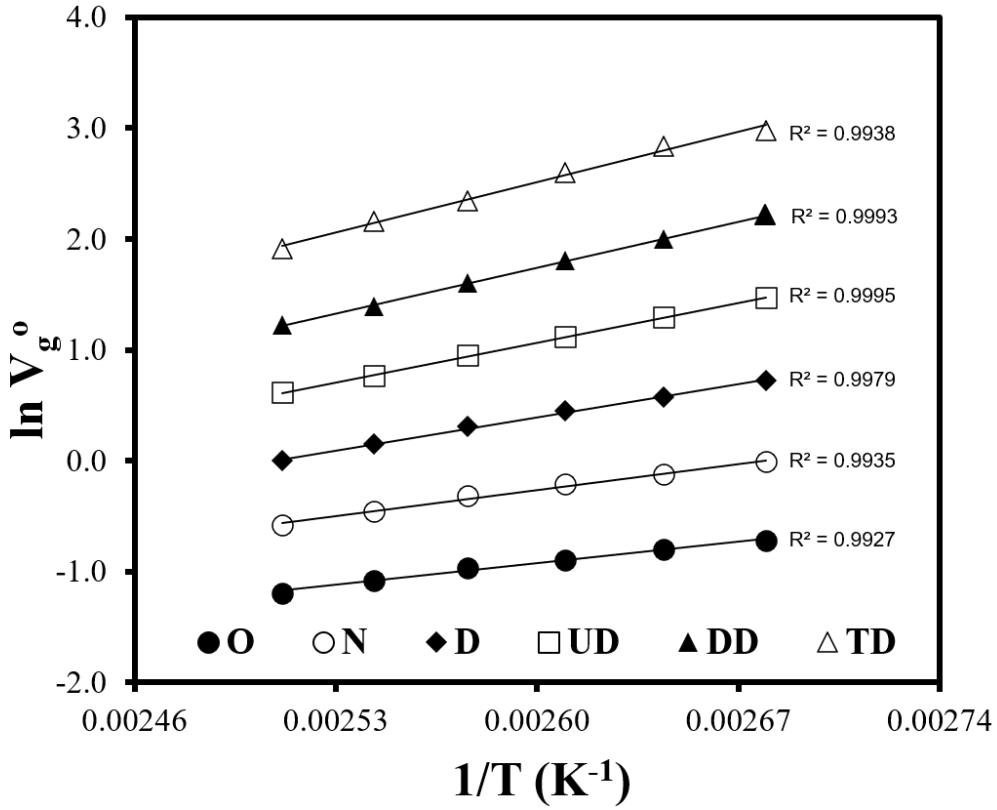

Figure 1. The retention diagrams of polar solvents on WB

Understanding the interaction parameters between polymers and solvents is essential for evaluating their miscibility and the thermodynamic behavior of polymer solutions. IGC has proven to be an effective technique for determining the thermodynamic properties of solvent vapors interacting with polymers.

Using Equations (3) and (4), the Flory–Huggins and equation-of-state interaction parameters were calculated, and the obtained values are presented in Tables 2 and 3, respectively.

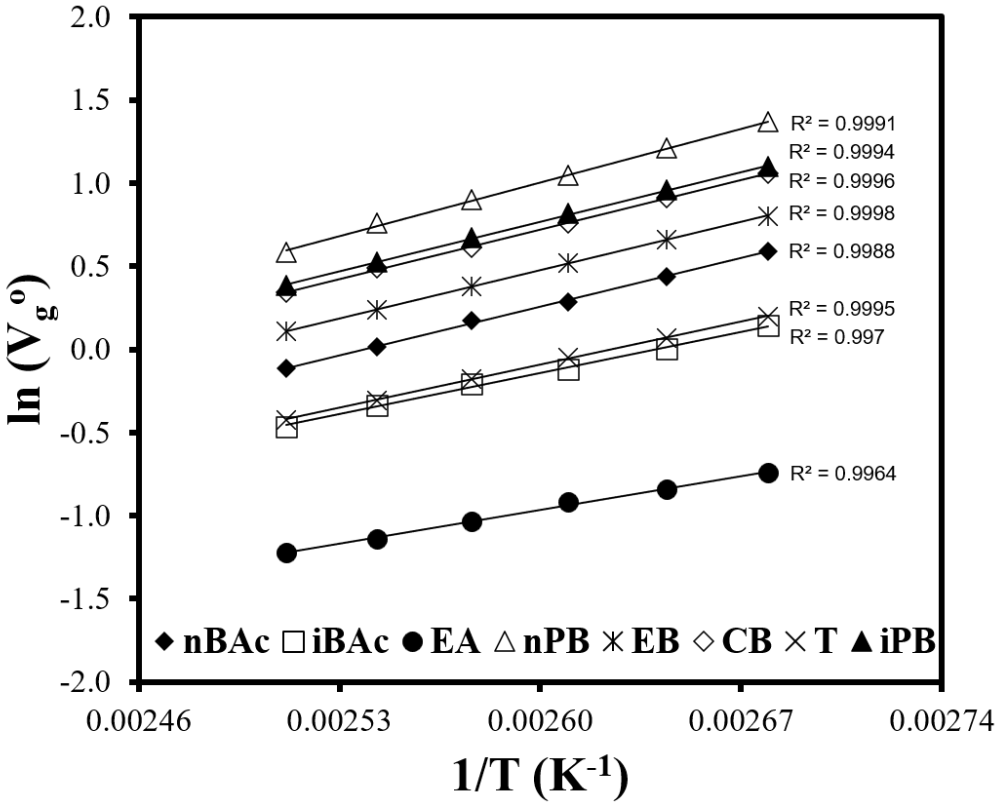

Figure 2. The retention diagrams of non-polar solvents on WB

Table 2. Flory–Huggins interaction parameters, χ_{12}^{∞}, for WB

T(K)	373.2	378.2	383.2	388.2	393.2	398.2
O	5.82	5.74	5.69	5.62	5.59	5.57
N	5.86	5.80	5.72	5.67	5.64	5.62
D	5.87	5.83	5.78	5.74	5.72	5.71
UD	5.88	5.85	5.82	5.79	5.79	5.76
DD	5.89	5.88	5.85	5.84	5.84	5.81
TD	5.89	5.78	5.79	5.80	5.77	5.80
EB	4.75	4.74	4.72	4.71	4.71	4.69
EA	4.70	4.67	4.62	4.61	4.60	4.56
nBA	4.65	4.64	4.63	4.60	4.60	4.59
IBA	4.78	4.77	4.73	4.68	4.67	4.66
nPB	4.82	4.80	4.79	4.78	4.76	4.78
iPB	4.81	4.79	4.76	4.75	4.74	4.74
CB	4.48	4.47	4.46	4.47	4.44	4.45
T	4.52	4.50	4.48	4.48	4.48	4.47

Standard uncertainty u is u(χ_{12}^{∞}) = 0.04

According to Flory–Huggins theory, a value of $\chi_{12}^{\infty} < 0.5$ indicates strong intermolecular interactions between polymer chains and solvent molecules, whereas $\chi_{12}^{\infty} > 0.5$ signifies weak interactions in dilute polymer solutions. As shown in Tables 2 and 3, all solvents examined at the studied temperatures behave as poor solvents for WB.

For alkane solvents, both χ_{12}^{∞} and χ_{12}^{*} generally increase with increasing carbon number at a given temperature. This trend can be attributed to dispersive interactions associated with $-CH_2-$ groups, which reduce polymer–solvent miscibility as chain length increases.

The χ_{12}^{∞} and χ_{12}^{*} values for alkylbenzenes are generally lower than those for alkanes, which can be attributed to the stronger interactions between aromatic compounds and the solvent arising from π-electron contributions.

The effective exchange energy parameter (χ_{eff}) was calculated using Equation (6), and the corresponding results are presented in Table 4. This parameter quantifies the change in contact energy when a polymer segment adjacent to another polymer segment is replaced by a solvent molecule. Higher χ_{eff} values indicate poorer solubility, whereas lower values suggest better solubility due to specific interactions between the solvent and the polymer.

Table 3. The equation-of-state interaction parameters, χ_{12}^{*}, for WB

T(K)	373.2	378.2	383.2	388.2	393.2	398.2
O	6.00	5.93	5.87	5.80	5.77	5.75
N	6.04	5.98	5.90	5.84	5.82	5.79
D	6.06	6.01	5.96	5.92	5.90	5.88
UD	6.07	6.03	6.00	5.97	5.96	5.93
DD	6.08	6.07	6.03	6.02	6.02	5.98
TD	6.09	5.97	5.98	5.99	5.95	5.97
EB	4.91	4.90	4.88	4.87	4.87	4.85
EA	4.91	4.88	4.83	4.83	4.82	4.79
nBA	4.83	4.82	4.81	4.78	4.78	4.77
IBA	4.97	4.95	4.92	4.87	4.86	4.85
nPB	4.98	4.96	4.95	4.94	4.92	4.94
iPB	4.98	4.95	4.92	4.91	4.90	4.90
CB	4.62	4.62	4.61	4.62	4.60	4.60
T	4.68	4.67	4.65	4.65	4.65	4.64

Standard uncertainty u is u(χ_{12}^{*}) = 0.04

Table 4. Effective exchange energy parameters of the solvents, $\chi_{eff}(j/cm^3)$, of WB

T(K)	373.2	378.2	383.2	388.2	393.2	398.2
O	159.01	158.87	159.12	159.03	159.98	161.16
N	144.47	144.63	144.31	144.58	145.69	146.55
D	132.62	133.15	133.40	134.01	135.10	136.28
UD	122.28	122.94	123.81	124.49	125.87	126.55
DD	113.41	114.51	115.19	116.32	117.73	118.25
TD	105.94	105.15	106.45	107.94	108.49	110.22
EB	174.49	176.04	177.63	179.19	181.35	182.79
EA	219.10	220.23	220.23	222.52	224.66	225.58
nBA	156.04	157.66	159.22	159.64	161.78	163.17
IBA	146.88	148.15	148.82	148.61	149.93	151.29
nPB	150.54	151.90	153.50	154.82	156.03	158.50
iPB	154.26	155.20	156.36	157.86	159.40	161.12
CB	199.39	201.53	203.85	206.52	208.02	210.71
T	193.55	195.28	196.98	199.02	201.67	203.45

Standard uncertainty u is u(χ_{eff}) = 2.5

The values of χ_{12}^{∞}, χ_{12}^{*}, and χ_{eff} indicate that all the selected solvents behave as poor solvents for WB within the temperature range of 373.2–398.2 K. Furthermore, the results obtained for χ_{12}^{∞}, χ_{12}^{*} and χ_{eff} are consistent with one another.

The values of $\Delta\bar{H}_v$ were calculated using Equation (10) and compared with the literature values, $\Delta\bar{H}_{vl}$. The results are presented in Table 5. Good agreement was observed for solvents whose boiling temperatures are close to the average temperature range investigated in the column. This comparison suggests that the thermodynamic properties determined in this study are reasonably reliable.

Table 5. The values of molar evaporation enthalpies ($\Delta\bar{H}_v$), molar evaporation enthalpies in literature ($\Delta\bar{H}_{vl}$) [24] partial molar sorption heats ($\Delta\bar{H}_1^S$), partial molar dissolution enthalpies at infinite dilution ($\Delta\bar{H}_1^\infty$), and boiling points for polar and non-polar solvents on WB.

Solvent	$\Delta\bar{H}_1^\infty$	$\Delta\bar{H}_1^s$	$\Delta\bar{H}_v$	$\Delta\bar{H}_{vl}$	Boiling points (°C)
O	3.1	-5.5	8.6	8.2	125.6
N	3.0	-6.6	9.6	8.8	151.0
D	2.2	-8.5	10.7	9.4	174.1
UD	1.6	-10.2	11.8	9.9	195.9
DD	1.1	-11.7	12.8	10.4	216.2
TD	1.1	-12.9	14.0	10.9	234.0
nBA	0.8	-8.3	9.1	8.6	126.0
iBA	1.7	-7.0	8.7	8.7	117.0
EA	1.4	-5.8	7.2	7.7	77.1
nPB	0.6	-9.2	9.8	9.1	159.0
iPB	0.9	-8.5	9.4	9.0	152.5
EB	0.7	-8.2	8.9	8.5	136.0
CB	0.3	-8.4	8.7	8.7	132.0
T	0.5	-7.4	7.9	7.9	110.6

The analysis of $\Delta\bar{H}_1^\infty$, $\Delta\bar{H}_1^S$, and $\Delta\bar{H}_v$ parameters is essential for understanding the sorption mechanism. The $\Delta\bar{H}_1^S$ values for solvent sorption on WB were determined from the slope of the linear plot of $\ln V_g^0$ versus $1/T$ over the temperature range of 373.2–398.2 K (Table 5). The partial molar enthalpy of mixing, $\Delta\bar{H}_1^\infty$, describes solvent–polymer interactions in the condensed phase. These values were obtained from the slopes of plots of $\ln \Omega_1^\infty$ versus $1/T$ within the studied temperature range using Equation (7). The sign and magnitude of $\Delta\bar{H}_1^\infty$ indicate whether the solubility process is exothermic (negative) or endothermic (positive) for the investigated solvents.

III. RESULTS AND DISCUSSIONS

The thermodynamic characterization of WB and the determination of their thermodynamic parameters are highly important for both industrial applications and contributions to scientific literature. In this study, the thermodynamic characterization of the WB was successfully performed, and its thermodynamic parameters were determined using IGC method, which is simple to apply, cost-effective, and capable of providing highly accurate results. IGC is used as a crucial analytical method in materials science, polymer technology, pharmaceutical research, and composite development studies by determining properties such as a material's surface energy, acid-base character, adsorption behavior, and polymer interactions. Therefore, IGC is one of the most valuable techniques for surface and interface characterization. The obtained Flory–Huggins interaction parameter (χ_{12}^∞), the equation-of-state interaction parameter (χ_{12}^*), and the effective exchange energy parameter (χ_{eff}) indicate that all investigated probe solvents act as poor solvents for WB. Besides, according to these parameters and enthalpy values, the solubility of WB in non-polar and polar probes was found to be endothermic.

REFERENCES

1. Atia Sharif HN, Rehman R, Mushtaq A, Rashid U (2016) Review on bioactive potential of Benzoin resin. Int J Chem Biochem Sci 10:106–110.
2. Hacini Z, Khedja F, Habib I, Kendour Z, Debba Z (2018) Evaluation of antibacterial and antioxidant activities of three types of benzoin resin. European Journal of Chemistry 9:408–411.

3. Katz E, García Fernandez C, Goloubinoff M (2002) Sumatra benzoin (Styrax spp.).
4. Evans WC, Evans D (2009) Trease and Evans' Pharmacognosy Chapter 19—Hydrocarbons and derivatives. (Sixteenth Edition); Eds 2009:173–193.
5. Abbott S (2018) IGC Science: Principles and Practice. Adscientis Paris, France 44–49.
6. Boudriche L, Calvet R, Hamdi B, Balard H (2012) Surface properties evolution of attapulgite by IGC analysis as a function of thermal treatment. Colloids and Surfaces A: Physicochemical and Engineering Aspects 399:1–10.
7. Erdogan Cakar A (2026) Physicochemical characterization of thermodynamic parameters and isomer separation of Hemin by inverse gas chromatography. Brazilian Journal Of Chemical Engineering 43(1):241-253.
8. Zunino F, Palacios M, Bowen P, Scrivener K (2024) Surface properties of clinker phases and clay minerals characterized by inverse gas chromatography (IGC) and their link to reactivity. Cement and Concrete Research 178:107458.
9. Voelkel A, Andrzejewska E, Limanowska-Shaw H, Andrzejewski M (2005) Acid–base surface properties of glass-ionomers determined by IGC. Applied surface science 245:149–154.
10. Cakar AE, Cakar F, Ocak H, Karavelioglu S, Eran BB, Cankurtaran O (2023) Determination of thermodynamic properties and phase transition temperatures of phenylbenzoate-based calamitic liquid crystals by inverse gas chromatography method. Phase Transitions 96:731–745.
11. Bolvari A, Ward TC, Koning P, Sheehy D (1989) Experimental techniques for inverse gas chromatography. In: ACS Publications.
12. Hu D, Wang Q, Li J, Chen Y, Muhammad F, Zhang Y, Yalikun N, Huang H (2024) Thermodynamic properties of TPAC-EG deep eutectic solvents: A study based on the IGC method with molecular simulations. Journal of Molecular Liquids 407:125120.
13. Farshchi N, Abbasian A, Larijani K (2018) Assessment of the thermodynamic properties of DL-p-mentha-1, 8-diene, 4-isopropyl-1-methylcyclohexene (DL-limonene) by inverse gas chromatography (IGC). Journal of Chromatographic Science 56:671–678.
14. Yurtcu Celik S, Erdogan Cakar A, Ugraskan V, Yazici O (2026) Investigation of thermodynamic properties of agar via inverse gas chromatography. Journal of Polymer Research 33:64.
15. Voelkel A, Strzemiecka B, Milczewska K, Okulus Z (2015) Inverse gas chromatographic examination of polymer composites. Open Chemistry13:000010151520150104.
16. Smidsrød O, Guillet J (1969) Study of polymer-solute interactions by gas chromatography. Macromolecules 2:272–277.
17. Flory P, Orwoll R, Vrij A (1964) Statistical thermodynamics of chain molecule liquids. I. An equation of state for normal paraffin hydrocarbons. Journal of the American Chemical Society 86:3507–3514.
18. Revelli A-L, Mutelet F, Jaubert J-N, Garcia-Martinez M, Sprunger LM, Acree Jr WE, Baker GA (2010) Study of ether-, alcohol-, or cyano-functionalized ionic liquids using inverse gas chromatography. Journal of Chemical & Engineering Data 55:2434–2443.
19. McGlashan M, Potter D (1951) An apparatus for the measurements of the second virial coefficient using glycerol. In Proc R Soc.: 448–456.
20. Shillcock IM, Price GJ (2004) Interactions of solvents with low molar mass and side chain polymer liquid crystals measured by inverse gas chromatography. The Journal of Physical Chemistry B 108:16405–16414.
21. Voelkel A, Strzemiecka B, Marek AA, Zawadiak J (2014) Inverse gas chromatography investigation of oxidized polyolefins: Surface properties. Journal of Chromatography A 1337:194–201.
22. Yilmaz F, Cankurtaran Ö (1998) A study on the parameters of exchange enthalpy, X12, and entropy, Q12, in the equation-of-state theory for some polymer-solvent pairs. Polymer 39:1243–1247.
23. Çakar F, Cankurtaran O (2005) Determination of secondary transitions and thermodynamic interaction parameters of poly (ether imide) by inverse gas chromatography. Polymer Bulletin 55:95–104.
24. Myers MN (1971) Gas chromatography, principles, techniques, and application (Littlewood, AB). In Book Gas chromatography, principles, techniques, and application (Littlewood, AB) (Editor ed. eds.). City: ACS Publications.